Energy, Mines and Resources Canada | Énergie, Mines et Ressources Canada

**CANMET**

Canada Centre for Mineral and Energy Technology | Centre canadien de la technologie des minéraux et de l'énergie

# THE MICROSTRUCTURE AND MECHANICAL PROPERTIES OF LOW-ALLOY Cr/Mo STEEL WELD METALS

J.T. MCGRATH
WELDING SECTION

JUNE 1986

PHYSICAL METALLURGY RESEARCH LABORATORIES

MICROMEDIA

35 pp

REPORT: PMRL 86-53(TR)

This document is an unedited interim report prepared primarily for discussion and internal reporting purposes. It does not represent a final expression of the opinion of the Canada Centre for Mineral and Energy Technology (CANMET)

Ce document est un rapport provisoire non-révisé et rédigé principalement pour fin de discussion et de documentation interne. Il ne représente nullement l'expression définitive de l'opinion du Centre canadien de la technologie des minéraux et de l'énergie (CANMET)

PHYSICAL METALLURGY RESEARCH LABORATORIES
REPORT PMRL 86-53(TR)

# THE MICROSTRUCTURE AND MECHANICAL PROPERTIES OF LOW-ALLOY Cr/Mo STEEL WELD METALS

by

J.T. McGrath*

## INTRODUCTION

This is a review of the factors controlling the microstructure and mechanical properties of weld metals of low-alloy, heat resistant, Cr/Mo and Cr/Mo/V steels. The range of individual elements in these steels include: Cr - up to 5%, Mo - up to 1.5%, and V - up to 0.3%.

The factors controlling the weld-metal microstructure and mechanical properties such as notch toughness and creep rupture strength will be discussed. Weld embrittlement during fabrication (reheat cracking) and in-service (temper embrittlement) will also be discussed.

It should be noted that most of the data in the literature are for 2.25 Cr-1 Mo weld metals. For other weld-metal compositions, in many instances, comments on the factors controlling microstructure and mechanical properties are based upon the available data from base-metal compositions.

*CANMET, Department of Energy, Mines and Resources Canada, Ottawa.

# 1. MICROSTRUCTURE OF Cr/Mo WELD METALS

The microstructure of the weld metals of Cr/Mo heat-resistant steels is reviewed as a function of composition, cooling rate and post-weld heat treatment (PWHT). The type and amount of transformation products and the type and morphology of alloy carbide particles will be identified.

## 1.1 CCT DIAGRAMS AND THE PREDICTION OF AS-DEPOSITED MICROSTRUCTURE

Although continuous-cooling transformation (CCT) diagrams based upon weld thermal histories are not readily available, the CCT diagrams for various Cr/Mo base-metal compositions are useful in predicting the transformation products in as-deposited weld metals of similar composition.

In the continuous cooling of as-deposited weld metals the cooling rates will be dependent primarily upon the energy input from the welding process. Typically, for energy inputs from 1.5 to 6 kJ/mm and assuming a weldment thickness of $\geq$50 mm, cooling rates range from 180 to 750°C/min (1). In Fig. 1 CCT diagrams are depicted for 0.5 Cr-0.5 Mo-0.25 V, 0.75 Cr-0.5 Mo, 1.25 Cr-0.5 Mo, 2.25 Cr-1.0 Mo and 3 Cr-1.5 Mo steels. The cooling range of 180 to 750°C/min, is indicated in each diagram. As shown in Fig. 1(a), 1(b) and 1(c) increasing the Cr level to 1.25% with Mo remaining at 0.5% does not significantly affect hardenability, and the as-deposited weld-metal microstructures should contain primarily a mixture of ferrite and bainite over the typical cooling range encountered during welding. The data of Kunitake et al. (5) indicated that the addition of Cr up to 3% had little effect on the critical cooling rate for ferrite formation. The addition of V slightly reduces hardenability with additions up to about 0.3% (3). The contribution of V as a carbide former in the PWHT condition will be discussed later. The major change in the hardenability of the Cr/Mo steels takes place when the amount of Mo is increased to $\geq$1.0% as shown in Fig. 1(d) and 1(e). This results in the formation of a totally bainitic structure when cooling after welding. Another important factor is that the bainitic transformation temperature for both the 2.25 Cr-1 Mo and the 3 Cr-1.5 Mo steels does not change appreciably over a wide cooling range. This means that the dimensions of the bainitic microstructure should not change with a reduction in cooling rate (increasing energy input).

The effect of C on the hardenability of Cr-Mo steels can be significant. In a study on 2.25 Cr-1 Mo base metal, Wada and Eldis (3) showed that the critical cooling rate for ferrite formation, $K_f$, decreased from 30°C/min to 3°C/min as the C content was increased from 0.11 to 0.31%. Using the CCT diagram produced from 2.25 Cr-1 Mo weld metal, Lundin et al. (6) showed that the bainite start transformation temperatures were 10 to 38°C lower for weld metal containing 0.12-0.13% carbon compared with that with 0.08-0.09% carbon.

## 1.2 CHARACTERIZATION OF AS-DEPOSITED MICRO-CONSTITUENTS

While the analysis of CCT diagrams for Cr/Mo steel compositions are useful in the prediction of the as-deposited weld-metal micro-constituents, the full characterization of weld-metal structures has been limited almost entirely to the 2.25 Cr-1 Mo composition. The features of the bainitic microstructure of 2.25 Cr-1 Mo will be described based upon the terminology of Torronen (7) and Kotilainen (8). They described the bainitic structure of a continuously cooled Cr-Mo-V alloy in terms of four grain units. As illustrated in Fig. 2, the prior austenite grain is divided into packets. These packets are elongated in shape and are separated by high-angle boundaries. Kotilainen (8) reported that the orientation relationship between neighbouring packets was usually a twin orientation. A group of packets forms a bundle. Individual packets are further divided into parallel laths. The lath boundaries inside a packet are always low-angle boundaries. The work of Naylor and Krahe (9) provides some insight into what controls the size of the bainite packets. This will be important later in explaining the fracture properties of Cr/Mo weld metals. Naylor and Krahe were able to vary the packet size in a 0.1 C 0.5 Mo/B steel by cooling test specimens over a range of cooling rates within the bainite transformation region of the CCT diagram shown in Fig. 3. Thus they found that the bainite packet dimensions decreased as the transformation temperature decreased (Fig. 4). If one extrapolates the relationship of packet width with transformation temperature to lower temperatures, the packet dimensions (2.4 to 3.7 μm) for a continuously-cooled (160-230°C/min) 2.8 Cr-0.6 Mo-0.3 V alloy (8) with a transformation temperature of 550°C agree reasonably well with the predicted packet size.

The bainitic microstructure observed in 2.25 Cr-1 Mo weld metal in the as-deposited and PWHT condition is shown typically in Fig. 5(a) from the work of Chandel et al. (10). Prior austenite grains within the columnar

region contain bundles of elongated packets. The width of individual packets was of the order of 3 to 6 μm. Assuming a bainite transformation start temperature of 535°C from the CCT diagram of Fig. 1(d) the bainite packet dimensions agree with those predicted from the linear relationship of Naylor and Krahe in Fig. 3. Transmission electron microscopy revealed that individual packets contained a parallel lath structure. As shown in Fig. 5(b) the lath width was <1 μm. Electron diffraction indicated that the packets were separated by high-angle boundaries while the misorientation across lath boundaries was very small, i.e., of the order of 1 to 2 degrees. The bainitic features observed in the 2.25 Cr-1 Mo weld metal were similar to those found by Kotilainen (8) in a continuously-cooled and tempered 2.8 Cr-0.6 Mo-0.3 V alloy. The identification of alloy carbides within the bainite structure will be discussed in the following section on the effect of PWHT.

Several studies of the microstructure of 2.25 Cr-1 Mo weld metal reported that the bainite packet size was sensitive to C content. Lundin et al. (6) evaluated the structure of shielded metal arc welds containing 0.024, 0.045, 0.091 and 0.13% C. All welds exhibited a fully bainitic structure in the as-deposited condition with the exception of the weld containing 0.024% C which contained traces of polygonal ferrite. Although the packet dimensions were not given, it was reported that the bainite structure became finer with increasing C content. The dilatometric studies performed by Lundin et al. (6) confirmed that the finer bainite likely resulted from a decrease in transformation temperature with the increase in C content. Studies by ITO et al. (11) and Chandel et al. (12) on weld metals deposited by the submerged-arc process also indicated that increasing the carbon level in the range of 0.06 to 0.11 resulted in a finer bainitic packet size.

Since the bainite transformation temperature for 2.25 Cr-1 Mo steel does not change over a wide range of cooling rates as indicated in the CCT diagram in Fig. 1(d), the dimensions of the as-deposited bainite microstructure should not change with cooling rate. To confirm this in weld metals, McGrath et al. (13) prepared a series of SAW welds with the same welding consumables but with the energy input varying from 1.5 to 6 kJ/mm. There was no significant change in the bainitic packet dimensions up to 4 kJ/mm, with a slight coarsening being observed at 5 and 6 kJ/mm. Typical bainite structures from this study are shown in Fig. 6.

The PWHT (typically 690°C for 25 h) can effect the as-deposited bainitic structure in some instances. Lundin et al. (6) observed that equiaxed ferrite grains replaced the lath-like packets after PWHT of a low-C (0.024) weld bainite microstructure. Swift (14) also reported some loss of acicularity of the bainite structure in low-carbon (0.055%) SAW welds after PWHT. However, there was little modification of the elongated products with PWHT in the higher carbon ($\geq$0.08) weld metals (6).

## 1.3 PWHT AND THE FORMATION OF ALLOY CARBIDES

The formation of alloy carbides as a result of PWHT has been studied in Cr/Mo base metals more extensively than in weld metals (15,16,17). The characterization of alloy carbides in weld metals has been restricted to 2.25 Cr-1 Mo (6,14,18). Therefore the intent is to provide an account of what is known about alloy carbide formation in 2.25 Cr-1 Mo weld metal. This will be followed by some general observations of the formation of carbides as a function of temperature and time in base metals with varying Cr and Mo contents. The last information may be useful in predicting which carbides are likely to form in weld compositions other than 2.25 Cr-1 Mo as a result of PWHT.

Lundin et al. (6) identified the type, morphology and location of alloy carbide particles in 2.25 Cr-1 Mo SMAW welds as a function of PWHT. The study was conducted in welds with a C level of 0.09% and PWHT of 25.5 h at 635°C and 25 h at 704°C. $M_3C$ carbides were observed in the as-deposited structure. As indicated in Table 1, $M_2C$ carbides were only formed after the lower temperature (635°C) PWHT. The $M_2C$ particles were needle-like in shape with a length of the order of 0.15 μm. The $M_2C$ carbides were located in the matrix. The more stable $M_7C_3$, $M_{23}C_6$ and $M_6C$ carbides were found in the matrix and at grain boundaries after both the low and high PWHT. These particles were globular in shape and more massive than the $M_2C$ carbides. A similar sequence in carbide formation was observed by Swift (14) in 2.25 Cr-1 Mo SAW welds.

The investigation of Tamaki et al. (17) traced the development of alloy carbides with increasing temperature and time in steels with varying Mo and Cr levels. The general observations of this study should be applicable to weld metals of comparable Mo and Cr levels. As shown in Fig. 7, for steels with 1% Mo, $Mo_2C$ formed over a wide temperature/time range for Cr levels up

to 1.1%. At higher levels of Cr, the formation of $Mo_2C$ became more restricted and $Cr_7C_3$ and $M_{23}C_6$ carbides were more prominent. When the level of Mo was reduced to 0.5%, the formation of $Mo_2C$ was much more limited as indicated in Fig. 8. For Cr additions of $\geq$1.8%, $Mo_2C$ did not form and $M_{23}C_6$ and $Cr_7C_3$ carbides were identified.

Baker and Nutting (15), found similar results to Tamaki et al. (17) for 2.25 Cr-1 Mo base metal. Ritchie et al. (19), in agreement with the findings of Tamaki, reported that by increasing the level of Cr to 3% in a 3 Cr-1 Mo-1 Ni steel, $M_{23}C_6$ carbides replaced the less stable $M_2C$, $M_3C$ and $M_7C_3$ carbides at lower temperatures and shorter times.

## 2. MECHANICAL PROPERTIES

As was the case in the analysis of weld-metal microstructure, the data on mechanical properties of Cr/Mo weld metals reside primarily with the 2.25 Cr-1 Mo composition. This section will examine the factors which control the notch toughness and creep rupture strength of 2.25 Cr-1 Mo weld metals, principally, and other Cr/Mo compositions depending upon the availability of information.

### 2.1 NOTCH TOUGHNESS

#### 2.1.1 2.25 Cr-1 Mo Weld Metal

The notch toughness property requirements of 2.25 Cr-1 Mo base metal and weld metal are most stringent when they are used in the fabrication of heavy-walled, large diameter reactor vessels for the gasification and liquefaction of coal (20) and the hydrotreating of heavy oils and tar sands bitumen (21). The base metal and weld metal must have sufficient notch toughness to provide resistance to in-service temper and hydrogen embrittlement. Weld-metal notch toughness requirements are typically 54 J at -40°C for heavy oil hydrotreatment vessels (21).

There have been several studies (10,11,14,22) of the notch toughness properties of 2.25 Cr-1 Mo weld metal deposited by the submerged-arc-welding process. Toughness data from these studies are listed in Table 2. All of the welds listed have been PWHT to a similar tempering parameter, i.e., 690°C for 10 to 26 h.

The low temperature resistance to brittle fracture is listed as the 54 J transition temperature. By comparing welds with an oxygen content ranging from 0.022 to 0.035% it should be noted that the transition temperature decreased as the C level of the weld increased. The effect of increasing C is to lower the bainite transformation temperature resulting in a finer bainitic packet size. The work of Torronen (7) and Kotilainen (8) has shown that the grain size unit that controls the resistance to cleavage fracture in a continuously cooled and tempered bainitic Cr-Mo-V steel was the bainitic packet size. The unit fracture length corresponded with the bainite packet size, suggesting that the finer the packet size the higher the resistance to cleavage fracture. Examination of fractured surfaces by Kotilainen revealed that the average cleavage facet size corresponded very well to the size of the bainitic packets. Similar fractographic evidence was found on the fracture surfaces of 2.25 Cr-1 Mo weld metal samples by Chandel et al. (10) and ITO et al. (11). As illustrated in Fig. 9 both cleavage facets and bainite packets had similar dimensions, i.e., the width was of the order of 3 to 6 μm. The fracture mechanism involved cleavage initiation and propagation across a bainite packet, with re-initiation taking place at each high-angled packet boundary. The low-angle lath boundaries within each packet [Fig. 5(b)] offer little resistance to crack propagation. It should be noted that there was no significant effect of energy input (Table 2) on the 54 J transition temperature. This would agree with the observations made previously in Section 1, that the bainitic transformation temperature and thus the bainitic packet size, does not change over a wide range of cooling rates (energy inputs).

The resistance to ductile fracture in 2.25 Cr-1 Mo weld metal, as indicated by the Charpy energy at 25°C (Table 2), was found to be dependent upon the volume fraction of inclusions. For the purpose of this review the volume fraction of inclusions is represented by the O + S content in Table 2. The energy at 25°C decreased as the O + S increased. The spherical oxysulphide inclusion particles act as sites for microvoid coalescence when the fracture mode is by ductile tearing. It is well known (23) that the control of oxygen content in SAW welds is through the selection of flux basicity. Those welds listed in Table 2 with oxygen contents $\leq$0.035% were deposited using high basicity fluxes. Finally, it should be noted that the effect of inclusions is not only to lower the Charpy upper shelf but also to shift the Charpy curve to nigher temperatures. Thus weld W2, listed in Table 2 as having the highest

O + S content, had the lowest energy at 25°C and the highest 54 J transition temperature.

### 2.1.2 3 Cr-1.5 Mo Weld Metal

The 3 Cr-1.5 Mo steel composition was designed for heavy section applications requiring improved hardenability and strength combined with good notch toughness properties. The data on notch toughness properties of weld metals is very limited. Recently, Swindeman et al. (24) prepared SAW welds in 100 mm thick plate of 3 Cr-1.5 Mo-0.1 V and 3 Cr-1.5 Mo-0.5 Ni composition. The weld-metal properties in the PWHT condition are listed in Table 3. Similar to the notch toughness properties of the 2.25 Cr-1 Mo weld metals, a significant improvement in toughness was achieved when the C content of the 3 Cr-1.5 Mo-0.1 V weld was increased from 0.05 (Welds A and C) to 0.084 (Weld B). Although there was no detailed analysis of weld microstructure a totally bainitic structure was reported. If one examines the CCT diagram for 3 Cr-1.5 Mo-0.1 V in Fig 1(e) the bainite transformation temperature is about 70°C lower than that of 2.25 Cr-1 Mo [Fig. 1(d)]. Thus a very fine bainite packet size is expected in 3 Cr-1.5 Mo-0.1 V weld metal which should be conducive to excellent low temperature toughness properties. Welds A and B had a high resistance to ductile fracture as evidenced by the high impact energy at 25°C. Although no analysis of O + S content was provided, the welds were made with a highly basic flux which should result in O levels $\leq$0.03% and acceptable low inclusion contents.

The 3 Cr-1.5 Mo-0.5 Ni weld metal with 0.12 C content had excellent low temperature properties combined with a higher strength as shown in Table 3. Although no CCT diagram was available, a fine bainitic microstructure was also expected for this composition.

### 2.1.3 Other Cr/Mo Weld Metals

Although, no published data exists on the notch toughness properties of the more dilute Cr/Mo weld metal compositions, the data of Murakami et al. (25) on continuously-cooled and tempered Cr/Mo base metals can provide guidelines for the expected notch toughness properties of weld metals of similar composition. The notch toughness properties of 1 Cr-0.5 Mo, 1.25 Cr-0.5 Mo, 2.25 Cr-1 Mo and 3 Cr-1 Mo steels austenitized, cooled at 100°C/min and PWHT are listed in Table 4. The notch toughness of the 1 Cr-0.5 Mo and 1.25 Cr-

0.5 Mo steels was less than that of the 2.25 Cr-1 Mo and 3 Cr-1 Mo steels. A further observation indicated that the 1 Cr-0.5 Mo steel had the lowest overall toughness of the 4 steels. The low temperature fracture resistance of these steels can be related to the micro-constituents after continuous cooling and PWHT. The relative amounts of the transformation products after cooling at 100°C/min can be estimated from the CCT diagrams in Fig. 1. As expected, the ferrite/pearlite mixture of the 1 Cr-0.5 Mo steel resulted in the lowest resistance to brittle fracture. The introduction of a fine bainitic constituent along with the ferrite in the 1.25 Cr-1 Mo improved the notch toughness. Finally, as discussed previously, the fine, totally bainitic structure of both the 2.25 Cr-1 Mo and 3 Cr-1 Mo steels provided excellent low temperature notch toughness properties. A similar ranking of notch toughness properties may be expected in as-deposited and PWHT weld metals of similar compositions.

## 2.2 CREEP RUPTURE STRENGTH

### 2.2.1 2.25 Cr-1 Mo Weld Metal

C.D. Lundin and co-workers have reviewed the literature on the stress rupture data for 2.25 Cr-1 Mo welds metals in addition to conducting their own research in an effort to provide an insight into the factors which control creep strength (26)(6). The creep strength was evaluated in terms of the effect of the following variables: (a) post-weld heat treatment temperature and time; (b) weld compositional variations, i.e., C content; (c) microstructural constituents and (d) welding process.

In order to include the test temperature and time to rupture factors in the analysis of stress rupture data of weld metals, Lundin plotted log stress vs Larson-Miller parameter graphs. The Larson-Miller parameter is expressed by the following equation:

$$LMP = (T)[C + \log(t_r)] \times 10^{-3}$$

where: T is the test temperature, K

C is a constant (C = 20 was used for all analyses)

$t_r$ is the rupture time in hours

If desired, the creep strength, expressed as the stress for 100,000 h rupture, can be calculated from the stress-LMP plots.

### 2.2.2 Effect of PWHT

The log S vs LMP plots for a range of temper parameters are shown in Fig. 10. The PWHT may range from 600 to 700°C for times up to 25 h. In constructing these graphs, Lundin et al. (6) have used the 2.25 Cr-1 Mo SMAW weld-metal stress rupture data from the literature in addition to their own experimental results from tests on SMAW welds. For a fixed value of the LMP, the rupture stress increased with decreasing temper parameter. Expressed in terms of the creep strength for 100,000 h rupture in Table 5, the improvement in creep strength with decreasing PWHT temper parameter is shown to be limited to test temperatures less than 480°C. At higher temperatures, additional tempering occurs during service thus reducing the creep strength to a level comparable with that obtained at higher temper parameters.

### 2.2.3 Effect of C Content

The effect of C on the 100,000 h creep strength is shown in Table 6. Increasing C addition to 2.25 Cr-1 Mo weld metal in the range of 0.02 to 0.12% increased the creep strength for PWHT temper parameters $< 20.8$. For PWHT with TP $> 20.8$, improved creep strength with increasing C addition was only found for levels up to 0.04%.

### 2.2.4 Effect of Microstructure

The changes in creep strength in 2.25 Cr-1 Mo weld metals that have been linked to PWHT and C addition can be explained on the basis of the influence that these two factors have on weld microstructure. For a weld metal containing 0.08-0.09% C, Lundin et al. (6) showed that the type and morphology of the carbides resulting from PWHT had a major effect on creep strength. For example, a PWHT of 635°C for 25.5 h (TP = 19.8) resulted in fine acicular $M_2C$ carbides which contributed to the superior creep strength. A PWHT of 704°C for 25 h (TP = 21.3) produced coarser, spheroidized carbides, identified as $M_{23}C_6$, $M_7C_3$, $M_6C$, which were not as effective as the $M_2C$ carbides in providing creep strength.

Although the major contribution of C to increased creep strength is in the formation of carbides (preferably $M_2C$), Lundin et al. (6) also indicated that the fineness of the bainite microstructure, controlled by C content, may be a secondary factor in determining the creep strength of 2.25 Cr-1 Mo weld metals particularly at higher PWHT (TP = 21.3). Higher C levels (0.08 to 0.13%) produced a fine tempered bainite after PWHT (TP = 21.3) while lower-C weld metals (0.02-0.03%) contained a coarser bainite with some indications of polygonal ferrite. Since the coarse, spheroidized carbides, produced by the higher PWHT, did not provide a strong contribution to creep strength, the presence of a fine bainitic structure will improve the strength in this instance.

### 2.2.5 Effect of Welding Process

Lundin et al. (26) investigated the creep strength of a series of welds made in 2.25 Cr-1 Mo steel using the SAW, ESW and SMAW processes. Stress rupture tests were performed after all welds had received the same PWHT, i.e., 704°C for 25 h. The 100,000-h rupture strength was determined from stress rupture tests conducted at temperatures of 454, 510, and 566°C. The data in Table 7 indicated that the creep strength of the SMA welds was slightly lower at all test temperatures when compared with the SAW and ESW welds. Further work by Lundin et al. (6), who included a wide range of 2.25 Cr-1 Mo weld data for several welding processes, indicated that the effect of using different arc welding processes on the creep strength of 2.25 Cr-1 Mo weld metals is not significant. This result is not unexpected when it is known that the characteristics of the bainite microstructure in 2.25 Cr-1 Mo weld metal are not significantly affected by the changes in cooling rate that may result from arc welding processes operating over a range of energy inputs.

## 2.2 OTHER Cr/Mo WELD METALS

Although data on the creep rupture strength of Cr/Mo weld metals other than 2.25 Cr-1 Mo is sparse, it is possible to speculate on the creep strength of these other compositions by considering the basic factors which control creep strength. Foremost is the role of alloy carbides. The formation of the fine, needle-like $M_2C$ carbides has been shown to be most beneficial for creep strength. It has been shown that $M_2C$ carbides are controlled by Mo and Cr content as well as tempering time and temperature. Another

important factor for the formation of $M_2C$ carbides is the presence of polygonal ferrite in the weld metal microstructure. Baker and Nutting (15) observed that $M_2C$ carbides form in ferrite much earlier in the tempering process, in contrast to their formation in bainite, and persist to higher tempering temperatures and times, being ultimately replaced by the more stable $M_6C$ carbide. This may be important to the creep strength of the 0.5 Cr-0.5 Mo-0.25 V, 1 Cr-0.5 Mo, and 1.25 Cr-0.5 Mo weld-metal compositions which can have a mixture of ferrite/pearlite/bainite in the as-deposited microstructure.

The formation of other alloy carbides such as $V_4C_3$ can be important for creep strength. V has a greater affinity for C than Mo. The data of Prescott and Braun (27) indicate that the 1000 h rupture strength of a 2 Cr-1 Mo steel at 550°C was increased by V additions up to 0.15%.

## 3. EMBRITTLEMENT

The weld metals of heat resistant Cr/Mo steels may experience various forms of embrittlement both during fabrication and in service. Two forms of embrittlement will be considered, (a) reheat cracking during PWHT and (b) temper embrittlement after extended hours in high-temperature service.

### 3.1 REHEAT CRACKING

Intergranular cracking can occur in Cr/Mo weld metals during PWHT. The susceptibility to reheat cracking is affected by alloying and residual elements (28). Alloying elements such as Cr, Mo and V, by forming carbides during PWHT in the temperature range of 500 to 600°C, can produce intergranular cracking by (a) strengthening the interior of grains, allowing creep deformation, the mechanism by which residual stresses are relaxed, to become concentrated at grain boundaries, and (b) by precipitating at grain boundaries and providing sites for nucleation of creep cavitation. The segregation of residual elements such as P, As, Sn and Sb to grain boundaries during PWHT can further weaken the boundaries leading to intergranular cracking.

The role of residual elements in reheat cracking, specifically, in 2.25 Cr-1 Mo weld metals, has been studied in several investigations (29,30, 31). Hunter (29) measured the change in ductility in SAW welds in the temperature range of 500-650°C. He found that intergranular cracking was located in

the coarse-grained columnar region of the weld and that the susceptibility to this cracking increased with increased weld copper content (0.25% max). The work of Wolstenholme (30), in reheat cracking studies of SAW and SMAW welds in 2.25 Cr-1 Mo also found that Cu, in addition to P, Sn, As, Sb contributed to reheat cracking susceptibility. He reported that SMAW welds were less prone to reheat cracking than SAW welds primarily because of the finer columnar grains in the SMAW as deposited region. Boniszewski (31) attempted to quantify the embrittling potency of the various residual elements by formulating a metal composition factor (MCF) as follows:

$$MCF = Si + 2\ Cu + 2\ P + 10\ As + 15\ Sn + 20\ Sb$$

The MCF factor can be equated with some appropriate parameter, i.e., reduction in ductility, representative of the onset of reheat cracking.

Tamaki et al. (17) sought to clarify the effect of alloy carbide precipitation on the susceptibility to reheat cracking in a range of Cr/Mo steels with varying Cr and Mo contents. Although the study was done on the HAZ, the results obtained should be applicable in principle to weld metals. It was concluded that those steels in which the $M_2C$ ($Mo_2C$) carbide formed preferentially during PWHT were more sensitive to reheat cracking. Steels in which $M_7C_3$ ($Cr_7C_3$) and/or $M_{23}C_6$ carbides formed were not sensitive to reheat cracking. The compositions and PWHT that produced $M_2C$ carbides were discussed in detail in Section 1 and are shown in Fig. 7 and 8.

## 3.2 TEMPER EMBRITTLEMENT

Cr/Mo steel weld metals operating for extended periods in the temperature range of 325 to 575°C can be subject to temper embrittlement. The embrittlement takes place as a result of segregation of residual elements such as P, As, Sb, and Sn to grain boundaries. Temper embrittlement is usually manifested by a shift of the Charpy impact ductile/brittle transition temperature to higher temperatures with fracture occurring along grain boundaries.

There have been empirical formulae developed for Cr/Mo plate steels to quantify the role of the various residual and alloying elements in the temper embrittlement phenomenon. Bruscato (32) formulated a relationship which embodied the effect of P, Sn, Sb and As as follows:

$$X = \frac{10\ P + 5\ Sb + 4\ Sn + As}{100}$$

Watanabe et al. (33) developed a formula called the J factor which emphasized the role of two key segregates, P and Sn and alloying elements, silicon and manganese which assist the embrittling process, the latter because of its tendency for cosegregation.

$$J = (Si + Mn)(P + Sn) \times 10^4$$

The factors which control temper embrittlement in Cr/Mo weld metals will be reviewed. While most of the data have been generated for 2.25 Cr-1 Mo weld metals, corresponding plate data will be used to comment on the temper embrittlement of other Cr/Mo compositions for which weld metal data were not available.

3.2.1 Factors Controlling Weld Metal Temper Embrittlement

Because temper embrittlement involves long-time exposure, laboratory step cooling treatments have been devised to simulate the service behaviour of the steel or weld metal. Grosse-Woerdemann and Dittrich (34) have tabulated (Table 8) three-step cooling treatments which are essentially similar. If the notch toughness requirement of Cr/Mo weld metals for petrochemical reactor vessels is 54 J at -40°C after PWHT, the toughness after step cooling is 54 J at -29°C. With this criterion, let us examine notch toughness data for some SAW and SMAW welds of 2.25 Cr-1 Mo steel after a step cooling embrittling treatment. As shown in Table 9, the Charpy energy at -29°C is listed as well as the shift in the Charpy transition curve, $\Delta$TT at 54 J, after step cooling. The value of $\Delta$TT, which ranged from 0 to 35°C, is a measure of the degree of embrittlement. There was no definite correlation between $\Delta$TT and the Bruscato and J factors. Thus these factors do not adequately describe the embrittling behaviour of the weld metals. A similar result was shown by Komizo (36) in plotting $\Delta$TT values against the J factor for SAW and SMAW 2.25 Cr-1 Mo welds.

The fact that the data in Table 9 show that only two of the welds met the notch toughness requirement of 54 J at -29°C after step cooling, indicates

that, in order to minimize temper embrittlement, the main priority, after ensuring a low level of residual elements, is to improve the weld notch toughness in the as-deposited and PWHT condition. Grosse-Woerdemann and Dittrich (34) suggested that one of the most important metallurgical actions to improve notch toughness is to increase the basicity of the SMAW electrode coating and the SAW flux. This action would reduce the weld-metal inclusion content and shift the Charpy transition curve to lower temperatures as discussed previously. They also suggest that manganese should not have the embrittling effect in weld metals as it is proposed to have in the plate steel. Manganese does not cosegregate with residual elements due to the rapid solidification and subsequent high cooling rates encountered by weld metals.

In commenting on the susceptibility of temper embrittlement in 1 Cr-0.5 Mo and 1.25 Cr-0.5 Mo weld metals, reference is given to the behaviour of the plate-steel compositions. The data of Murakami et al. (25,37) indicated that no temper embrittlement was found in 1 Cr-0.5 Mo steel. They observed that temper embrittlement only occurred in 1.25 Cr-0.5 Mo steel when the Si content was >0.5%, the P + Sn level was >0.03%, and if the cooling rate following austenization was high enough to increase the bainitic fraction in the mixed structure of ferrite, pearlite and bainite. Whether these observations on temper embrittlement would apply to weld metals remain to be proven experimentally.

## 4. CONCLUSIONS

1. The microstructure of as-deposited Cr/Mo and Cr/Mo/V weld metals is dependent upon composition and cooling rate. For a cooling range of 180 to 750°C/min and a fixed level of Mo (0.5%) increasing the Cr level up to 1.25% should result in an as-deposited weld-metal microstructure of ferrite, pearlite and bainite with bainite replacing pearlite at the highest Cr addition. When the Mo is raised to 1.0% and Cr added in the range of 2.25 to 3% the hardenability increases resulting in a totally bainitic structure in the as-deposited weld metal over a wide range of cooling rates (energy input).

2. Post-weld heat treatment produces a range of alloy carbide precipitates depending upon the temperature, and Mo and Cr levels. The formation of

fine, needle-like $M_2C$ carbides are formed at lower temperatures and increasing Mo and decreasing Cr additions. The more stable globular $M_7C_3$, $M_{23}C_6$ and $M_6$ particles form at higher temperatures and increasing Cr content.

3. Weld-metal mechanical property data are limited primarily to the 2.25Cr-1Mo composition. For high notch toughness applications such as heavy-wall hydrotreatment reactor vessels, optimum notch toughness results from a weld-metal microstructure containing a fine bainitic structure combined with a low inclusion content. This microstructure results from maintaining the carbon content of the weld metal at about 0.1% and the O + S level $\leq$0.03%. Improved creep rupture strength of 2.25Cr-1Mo weld metal is favoured by a low temperature PWHT, increasing carbon content up to 0.12%, and a high proportion of $M_2C$ type carbide precipitates.

4. Two forms of weld-metal embrittlement can occur during fabrication and in service. The susceptibility to intergranular reheat cracking during PWHT increases with the preferential formation of $M_2C$ type carbides, and the presence of residual elements such as P, Sn, As and Sb. Temper embrittlement, which takes place after long-time exposure to service temperatures in the range of 325 to 575°C, is controlled by the segregation of the residual elements P, As, Sb and Sn to grain boundaries. In addition to lowering the level of residual elements, the reduction of the tendency for temper embrittlement is accomplished by improving the notch toughness of the weld metal in the as-deposited and PWHT condition.

## REFERENCES

1. Graville, B.A., Principles of Cold Cracking in Welds, Dominion Bridge Co. publ., Montreal (1975).

2. Atkins, M., Atlas of Continuous Cooling Transformation Diagrams for Engineering steels, British Steel Corp. (1977).

3. Wada, T. and Eldis, G.T., Transformation Characteristics of 2.25 Cr-1 Mo Steel; ASTM STP 755, ASTM, p. 343, (1982).

4. Wada, T. and Cox, T.B., A new 3 Cr-1.5 Mo steel for Pressure Vessel Applications, Research on Chrome-Moly Steels, MPC 21, ASME, p. 77, (1984).

5. Kunitake, T., Yukitoshi, T., Yoshikawa, K., and Ohtani, H., Sumitomo Kinzoku, 22, (2), p. 189, (1970).

6. Lundin, C.D., Kelley S.C., Menon, R. and Kruse B.J., Stress Rupture Behaviour of PWHT 2.25 Cr-1 Mo Weld Metal, Welding Research and Engineering Group, Materials Science and Engineering Dept., University of Tennessee, Report, Jan. (1986).

7. Torronen, K., Microstructural Parameters and Yielding in Quenched and Tempered Cr-Mo-V Pressure Vessel Steel, Technical Research Centre of Finland, Publ. 22 (1979).

8. Kotilainen, H., The Micromechanisms of Cleavage Fracture and Their Relationship to Fracture Toughness in a Bainitic Low Alloy Steel, Technical Research Centre of Finland, Publ. 23 (1980).

9. Naylor, J.P. and Krahe, P.R., The Effect of The Bainite Packet Size on Toughness, Met. Trans. A, 5, p. 1699 (1974).

10. Chandel, R.S., Orr, R.F., Gianetto, J.A., McGrath, J.T., Patchett, B.M. and Bicknell, A.C., The Microstructure and Mechanical Properties of Narrow Gap Welds in 2.25 Cr-1 Mo Steel, IIW Doc. IX-1355-85 (1985).

11. ITO, Y., Nakaniski, M., Katsumoto, N. and Tsumura, H., Improvement of Toughness and Reduction of Temper Embrittlement in 2.25 Cr-1 Mo Weld Metal, The Sumitomo Search, No. 30, p. 41 (1985).

12. Chandel, R.S., Orr, R.F., Gianetto, J.A., McGrath, J.T. and Wright, B., Some Factors Affecting the Mechanical Properties of SAW Narrow Gap Welds, Proc. of Int. Conf. Welding for Challenging Environments, ASM/WIC, Toronto, (1985).

13. McGrath, J.T., Orr, R.F. and Gianetto, J.A., Unpublished results (1986).

14. Swift, R.A. and Rogers, H.C., Embrittlement of 2.25 Cr-1 Mo Steel Weld Metal by Postweld Heat Treatment, Weld, J., 52 (4), Res. Suppl. p. 145-S (1973).

15. Baker, R.G. and Nutting, J., The Tempering of 2.25 Cr-1 Mo Steel after Quenching and Normalizing, JISI, 192, p. 257, (1959).

16. Shaw, B.J., A Study of Carbides Formed in Low Alloy Cr-Mo Steels, Research on Chrome-Moly Steels, MPC 21, ASME, p. 117 (1984).

17. Tamaki, K., Suzuki, J. and Nakaseko, Y., Effect of Molybdenum Carbide on Reheat Cracking Sensitivity of Cr-Mo Steels, IIW Doc. IX-1159-80 (1980).

18. Gooch, D.J., The Relationship Between Creep Resistance and Carbide Distribution in 2.25 Cr-1 Mo Weld Metals, CEGB Rep. RD/L/N33/78 (1978).

19. Ritchie, R.O., Parker, E.R., Spencer, P.N. and Todd, J.A., A New series of Advanced 3 Cr-Mo-Ni Steels for Thick Section Pressure Vessels in High Temperature and Pressure Hydrogen Service, J. of Mat. for Energy Systems, 6 (3) p. 151 (1984).

20. Swindeman, R.W., Thomas, R.D., Nanstad, R.K. and Long, C.J., Assessment of the Need for an Advanced High-Strength Cr-Mo Steel for Construction of Gasifier Pressure Vessels, Oak Ridge National Laboratory report, ORNL/TM-8873 (1984).

21. Knight, R.F., Tyson, W.R., Lavigne, M.J., McGrath J.T. and Boyd, J.D., Materials for Hydrogenation Vessels, Proc. Conf. Materials to Satisfy the Energy Demand, ASM, Vancouver (1980).

22. Baach, H. and Scholz, E., The Effect of Simulated Heat Treatments on the Mechanical Properties of 2.25 Cr-1 Mo Type Weld Metals, Oerlikon Schweissmitteilungen, 96/97, p. 14 (1981).

23. Taylor, L.G., and Farrar, R.A., Metallurgical Aspects of the Mechanical Properties of SAW Weld Metal, Weld. and Met. Fab., May, p. 305 (1975).

24. Swindeman, R.N., King, J.F. and Nanstad, R.K., Final Report on 3 Cr-1.5 Mo Steels for Gasifier Pressure Vessel Construction, Oak Ridge National Laboratory Report ORNL/TM-9731 (1985).

25. Murakami, Y., Watanabe, J. and Mima, S., Heavy Section Cr-Mo Steels for Hydrogenation Services; Canadian Conference of Metallurgists, 1978.

26. Lundin, C.D., Kruse, B.J. and Pendley, M.R., High Temperature Properties of 2.25 Cr-1 Mo Weld Metal, WRC Bulletin 227 (1982).

27. Prescott, G.R. and Braun, C.F., Update on Modified 2.25 Cr-1 Mo and 3 Cr-Mo Alloys, MPC, HPV-7 (1983).

28. Dhooge, A., Dolby, R.E., Sebille, J., Steinmetz, R. and Vinckier, A.G., A Review of Work Related to Reheat Cracking in Nuclear Reactor Pressure Vessel Steels, Int. J. Pres. Ves. and Piping 6, p. 329 (1978).

29. Hunter, A.N.R., Reheat Cracking in 2.25 Cr-1 Mo SAW Weld Metal, Metal Const., Part 1, April, p. 198 (1982), Part 2, May, p. 266 (1982).

30. Wolstenholme, D.A., Transverse Cracking on Reheating of 2 Cr-Mo SAW Weld Metal, CEGB Report R/M/N868 (1976).

31. Boniszewski, T., Reheat Cracking in 2.25 Cr-1 Mo SAW Weld Metal, Metal Const., Sept., p. 495 (1982).

32. Bruscato, R., Temper Embrittlement and Creep Embrittlement of 2.25 Cr-1 Mo SMAW Weld Deposits, Weld. J., 49 (4), p. 148-5 (1970).

33. Watanabe, J., Shindo, Y., Murakami, Y., Adachi, T., Ajiki, S. and Miyano, K., Temper Embrittlement of 2.25 Cr-1 Mo Pressure Vessel Steel, ASME 29th Petroleum Engineering Conf. Dallas (1974).

34. Grosse-Woerdemann, J. and Dittrich, S., Prevention of Temper Embrittlement in 2.25 Cr-1 Mo Weld Metal, Metal Progress, July, p. 43 (1982).

35. Chandel R.S., McGrath, J.T., Knight, R.F., Gianetto, J.A., and Orr R.F., Mechanical Properties of 2.25 Cr-1 Mo Welds Deposited by SAW-Narrow Gap Process, J. of Mat. for Energy Systems, 7, (2), p. 137 (1985).

36. Komizo, Y., A Review on Reversible Temper Embrittlement in Cr-Mo steel Weld Metals, IIW Doc. IX-1321-84 (1984).

37. Murakami, Y., Nomura, T., and Watanabe, J., Heavy-Section 2.25 Cr-1 Mo Steel for Hydrogenation Reactors, ASTM STP 755, ASTM, p. 383 (1982).

Table 1 - Identification of alloy carbides in 2.25 Cr-1 Mo weld metal (6)

| Carbide | 635°C, 25.5 h | 704°C, 25 h |
|---|---|---|
| $M_2C$ | M | NF |
| $M_7C_3$ | M,b | M,b |
| $M_{23}C_6$ | B,m | B,m |
| $M_6C$ | M | M |

M - matrix location

B - grain boundary location

Capital letter denotes predominent location

Table 2 - The notch toughness of 2.25 Cr-1 Mo SAW weld metals

| Weld | Tempering parameter* | Energy input, kJ/mm | Yield strength, MPa | 54J transition temperature, °C | Impact energy at 25°C, J | C % | S % | O % |
|---|---|---|---|---|---|---|---|---|
| 1 | 20.2 | 2.0 | 492 | -48 | 213 | 0.10 | 0.009 | 0.026 |
| 2 | 20.2 | 2.0 | 469 | -10 | 98 | 0.06 | 0.011 | 0.085 |
| 3 | 20.2 | 2.0 | 456 | -60 | 258 | 0.10 | 0.007 | 0.022 |
| 4 | 20.2 | 2.0 | 435 | -30 | 240 | 0.075 | 0.005 | 0.029 |
| 5 | 20.6 | 4.3 | - | -23 | - | 0.06 | 0.006 | 0.054 |
| 6 | 20.6 | 4.3 | - | -50 | - | 0.11 | 0.004 | 0.025 |
| 7 | 20.6 | 4.3 | - | -37 | 176 | 0.08 | 0.005 | 0.035 |
| 8 | 20.6 | 4.3 | - | -33 | 152 | 0.08 | 0.004 | 0.047 |
| 9 | 20.4 | 1.8 | 456 | -37 | 122 | 0.055 | 0.021 | 0.069 |
| 10 | 20.4 | 1.9 | 468 | -28 | 167 | 0.076 | 0.007 | ~0.025 |

* $TP = T\ (20 + \log t) \times 10^{-3}$

where T = tempering temperature, K

t = tempering time, h.

Source of data

Welds 1 + 4 ref. 10

Welds 5 + 8 ref. 11

Weld 9 ref. 14

Weld 10 ref. 22

Table 3 - The notch toughness of 3 Cr-1.5 Mo SAW welds (24)

| Weld | Tempering parameter | Energy input, kJ/mm | Yield strength, MPa | 54J transition temperature, °C | Impact energy at 25°C, J | C % | V % | Ni % |
|---|---|---|---|---|---|---|---|---|
| A | 19.9 | 2.2 | 556 | -27 | 215 | 0.050 | 0.074 | - |
| B | 19.6 | 2.1 | 626 | -53 | 220 | 0.084 | 0.082 | - |
| C | 20.1 | 3.1 | 490 | -15 | 160 | 0.054 | 0.092 | - |
| D | 19.6 | 3.4 | 647 | -53 | 147 | 0.12 | - | 0.50 |

Table 4 - The notch toughness of Cr/Mo base plate (25)

| Steel | Microstructure | Tempering parameter | Impact energy |
|---|---|---|---|
| 1 Cr-0.5 Mo | ferrite + pearlite | 19.7 | 157 J at 0°C |
| 1.25 Cr-0.5 Mo | ferrite + bainite | 19.7 | 236 J at 0°C |
| 2.25 Cr-1 Mo | bainite | 20.2 | 236 J at -20°C |
| 3 Cr-1 Mo | bainite | 19.7 | 206 J at -10°C |

Table 5 - Creep rupture strengths of 2.25 Cr -1 Mo SMA weld metal as function of temper parameter and test temperature (6)

| Temper parameter | Stress for $10^5$ hour rupture (MPa) | | | | | |
|---|---|---|---|---|---|---|
| | 399°C | 427°C | 454°C | 482°C | 510°C | 538°C |
| TP < 17.8 | 624 | 458 | 260 | - | - | - |
| 17.8 < TP < 20.1 | 372 | 306 | 237 | 179 | 127 | 88 |
| 20.1 < TP < 20.8 | 327 | 265 | 206 | 159 | 116 | 84 |
| TP > 20.8 | 254 | 209 | 163 | 125 | 91 | 65 |

Table 6 - Creep rupture strength of 2.25 Cr-1 Mo SMA weld metal as a function of temper parameter, test temperature and carbon content (6)

| Temper Parameter | C Content | Stress for $10^5$ hour rupture (MPa) | | | | | |
|---|---|---|---|---|---|---|---|
| | | 399°C | 427°C | 454°C | 482°C | 510°C | 538°C |
| 17.8 < TP < 20.1 | 0.02 < C < 0.04 | - | - | - | - | 13.2 | 9.4 |
| | 0.04 < C < 0.08 | - | - | - | 24.5 | 19.8 | 14.7 |
| | 0.08 < C < 0.12 | 51.0 | 44.3 | 35.3 | 26.6 | 18.2 | 12.0 |
| | C > 0.12 | 53.7 | 45.7 | 37.8 | 31.3 | - | - |
| 20.1 < TP < 20.8 | 0.04 < C < 0.08 | 46.9 | 38.0 | 29.1 | 22.0 | 15.6 | 11.0 |
| | 0.08 < C < 0.12 | 50.9 | 41.5 | 32.6 | 25.5 | 19.1 | 14.3 |
| TP > 20.8 | 0.02 < C < 0.04 | 31.3 | 25.5 | 19.7 | 15.2 | 11.1 | 8.1 |
| | 0.04 < C < 0.08 | 38.3 | 31.3 | 24.6 | 19.5 | 14.8 | 11.3 |
| | 0.08 < C < 0.12 | 38.2 | 31.8 | 25.1 | 19.4 | 14.1 | - |
| | C > 0.12 | 39.8 | 32.5 | 25.2 | 19.3 | 13.9 | - |

Table 7 - The effect of welding process on the creep rupture strength of 2.25 Cr-1 Mo weld metal (26)

| Welding process | C content % | Test temperature stress (MPa) | | |
|---|---|---|---|---|
| | | 454°C | 510°C | 566°C |
| SAW | 0.12 | 258 | 154 | 83 |
| ESW (Q & T) | 0.11 | 252 | 162 | 90 |
| SMAW | 0.12 | 206 | 105 | 56 |

Table 8 - Three step cooling embrittling treatments[1]

| Temperature, °C | Exposure time, h | | | Cooling rate, °C/h | | |
|---|---|---|---|---|---|---|
| | GE | Braun | Socal | GE | Braun | Socal |
| 595 | 1 | 1 | 1 | 6 | 6 | 6 |
| 540 | 15 | 15 | 15 | 6 | 6 | 6 |
| 525 | 24 | 24 | 24 | 6 | 6 | 6 |
| 495 | 60 | 60 | 60 | 3 | 3 | 6 |
| 470 | 125 | 100 | 100 | 28 | 28 | 28 |
| 315 | - | - | - | Air cool | Air cool | Air cool |

[1]GE = General Electric Co., Braun = C.F. Braun & Co.
Socal = Standard Oil Co. of California

Table 9 - Temper embrittlement of 2.25 Cr-1 Mo weld metals

| Weld | Impact energy, J, at -29°C | Δ TT at 54 J, °C | Bruscato factor | J factor |
|---|---|---|---|---|
| SAW 1 | 60 | 15 | 18.9 | 175 |
| SAW 2 | 12 | 30 | 12.8 | 162 |
| SAW 3 | 125 | 8 | 10.9 | 86 |
| SAW 4 | 4 | 35 | 12.3 | 277 |
| SAW 5 | 13 | 0 | 16.3 | 140 |
| SAW 6 | 10 | 10 | 13.3 | 118 |
| SAW 7 | 41 | 27 | 10.4 | 116 |
| SAW 8 | 28 | 17 | 28.7 | 193 |

Source of data: SAW 1 + SAW 6 ref 36
SMA 7, 8 ref 35

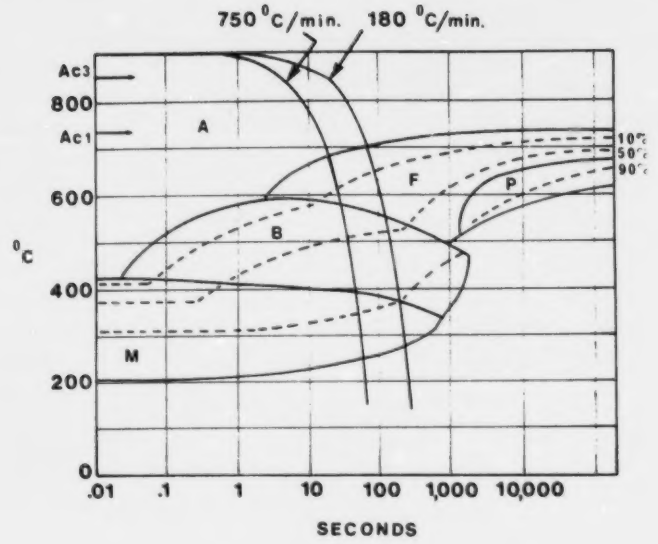


Fig. 1(a) - CCT diagram for 0.5 Cr-0.5 Mo-0.25 V (2)(neg 14430)

| C | Si | Mn | Cr | Mo | Ni | V |
|---|---|---|---|---|---|---|
| 0.12 | 0.25 | 0.55 | 0.40 | 0.60 | 0.15 | 0.25 |

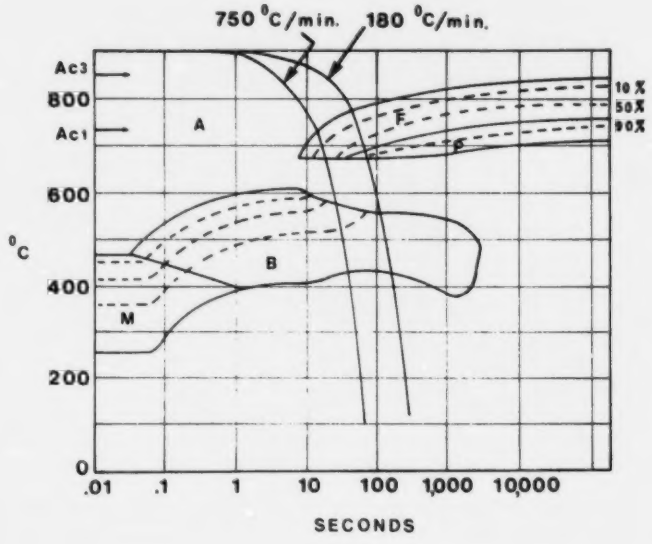


Fig. 1(b) - CCT diagram for 0.75 Cr-0.5 Mo (2) (neg 14483)

| C | Si | Mn | Cr | Mo | Ni |
|---|---|---|---|---|---|
| 0.12 | 0.30 | 0.45 | 0.85 | 0.60 | 0.16 |

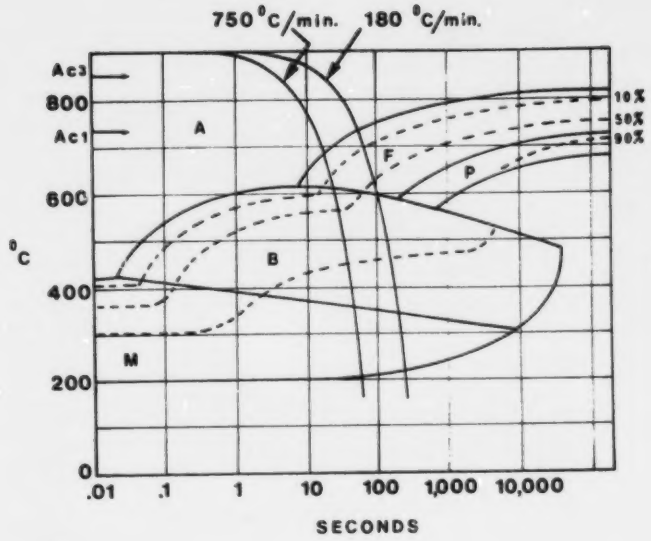


Fig. 1(c) - CCT diagram for 1.25 Cr-0.5 Mo (2) (neg 14482)

| C | Si | Mn | Cr | Mo |
|---|---|---|---|---|
| 0.15 | 0.30 | 0.60 | 1.25 | 0.50 |

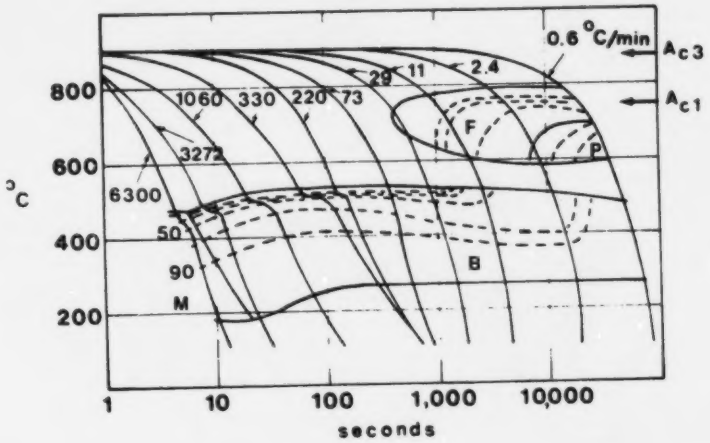


Fig. 1(d) - CCT diagram for 2.25 Cr-1 Mo (3) (neg 14479)

| C | Si | Mn | Cr | Mo |
|---|---|---|---|---|
| 0.11 | 0.22 | 0.58 | 2.17 | 0.95 |

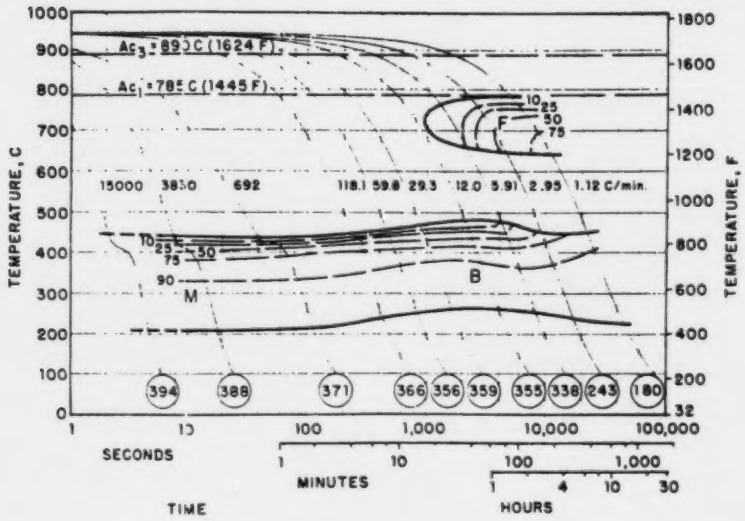


Fig. 1(e) - CCT diagram for 3 Cr-1.5 Mo (4) (neg 14488)

| C | Si | Mn | Cr | Mo | Ni | V |
|---|---|---|---|---|---|---|
| 0.12 | 0.27 | 0.84 | 2.86 | 1.48 | 0.14 | 0.09 |

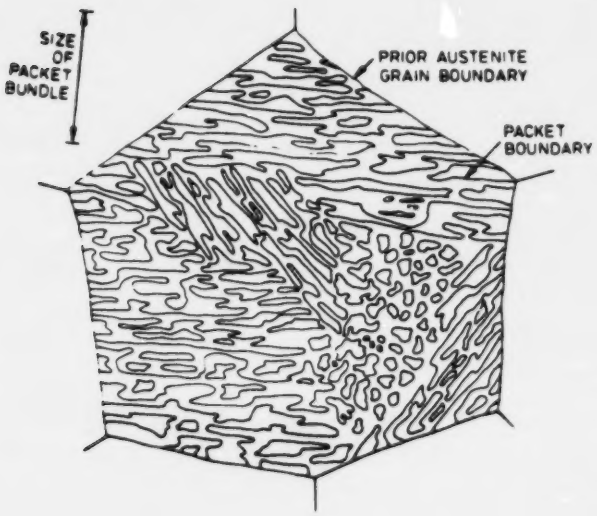


Fig. 2 - Schematic characterization of bainitic microstructure (8) (neg 14435)

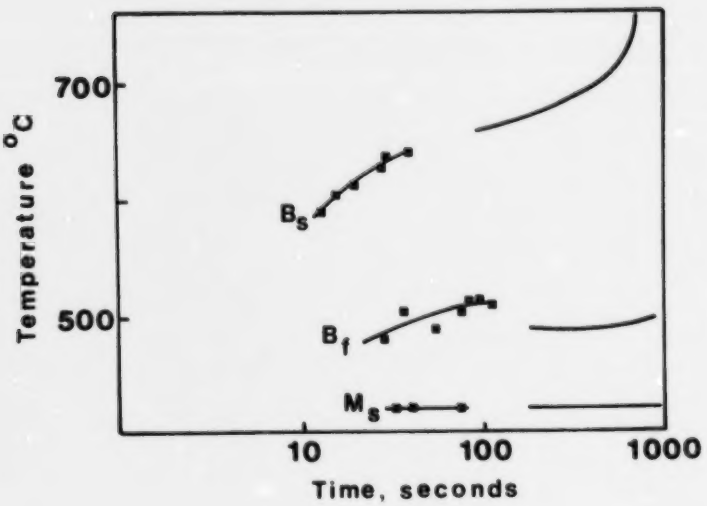


Fig. 3 - CCT diagram for 0.1 C-0.5 Mo-B steel (9) (neg 14532)

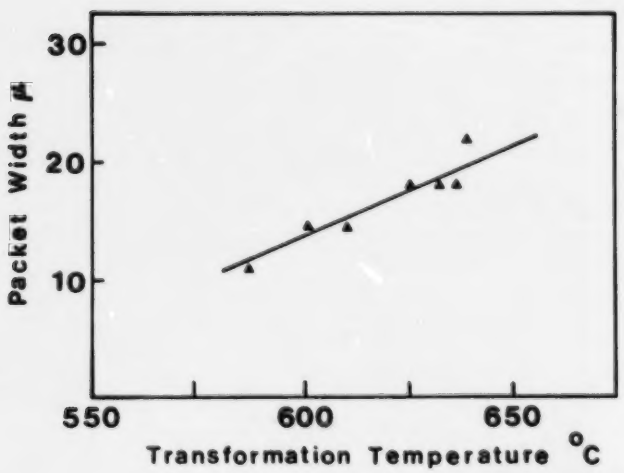


Fig. 4 - Variation of the bainitic packet width with transformation temperature (9) (neg 14486)

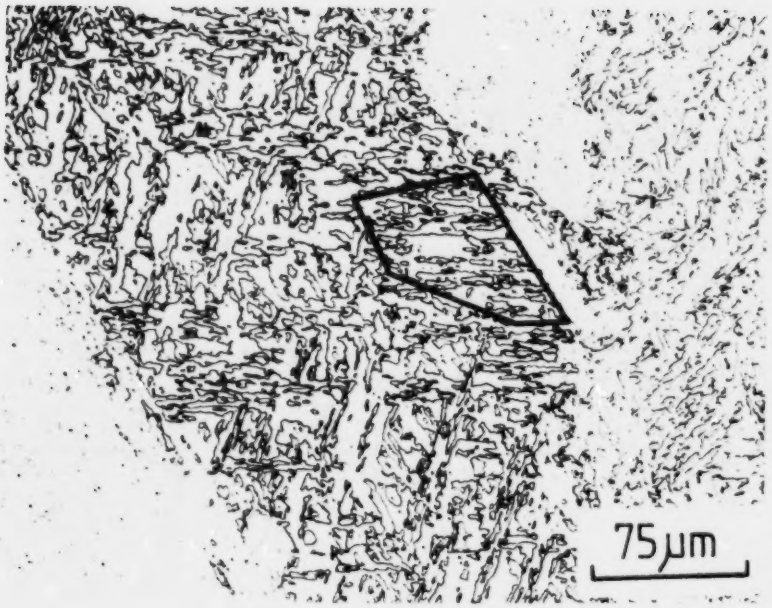


Fig. 5(a) - Bainitic structure of 2.25 Cr-1 Mo SAW weld metal. Packet bundle is outlined (10) (12264)

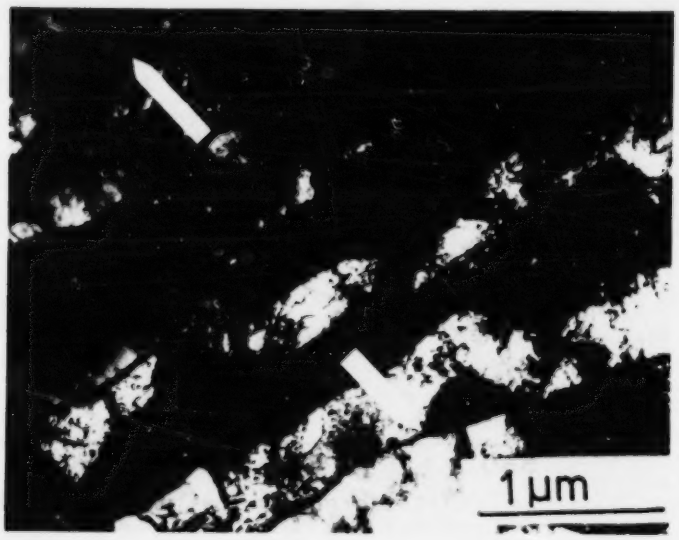


Fib. 5(b) - Structure of bainite packet. High-angle packet boundaries are indicated. Low-angle lath boundaries are contained within a packet (10). (neg 12280)

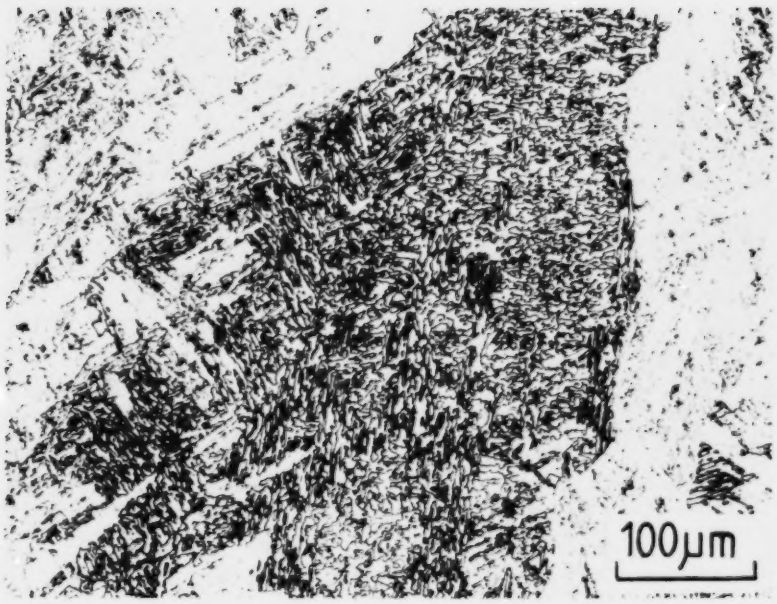


Fig. 6(a) - Bainitic structure of 2.25 Cr-1 Mo SAW weld metal deposited at 2 kJ/mm energy input (13). (neg 14583)

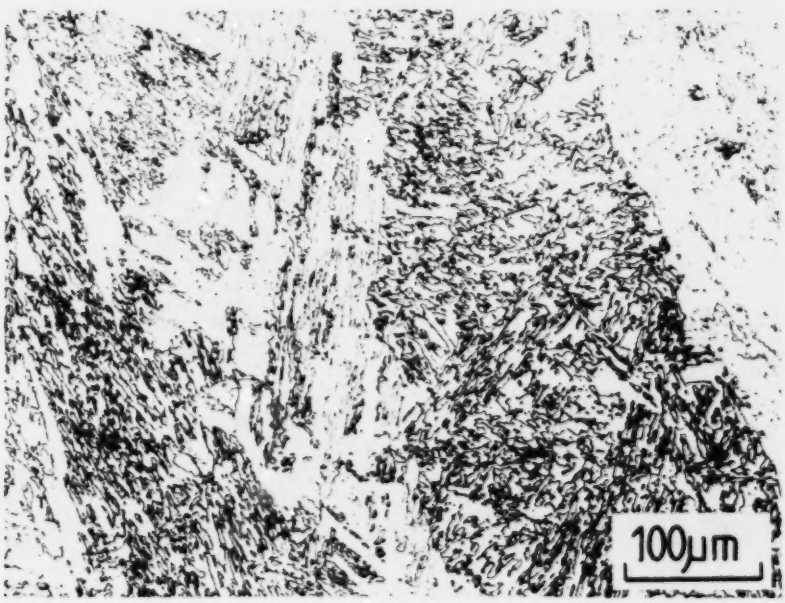


Fig. 6(b) - Bainitic structure of 2.25 Cr-1 Mo SAW weld metal deposited at 6 kJ/mm energy input (13). (neg 14582)

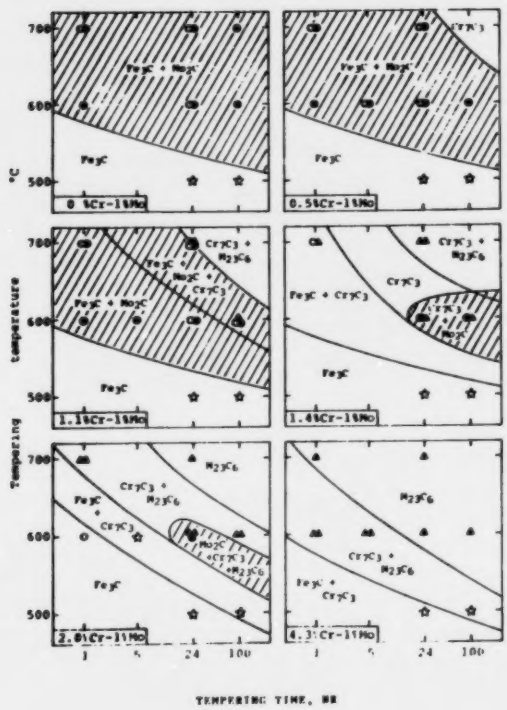


Fig. 7 - Carbide types present in Cr-1 Mo steels shown in the tempering-time diagram (17). (neg 14481)

Note: ° $Fe_3C$, ° $Mo_2C$, Δ $Cr_7C_3$, Δ $M_{23}C_6$,
* no diffraction pattern.

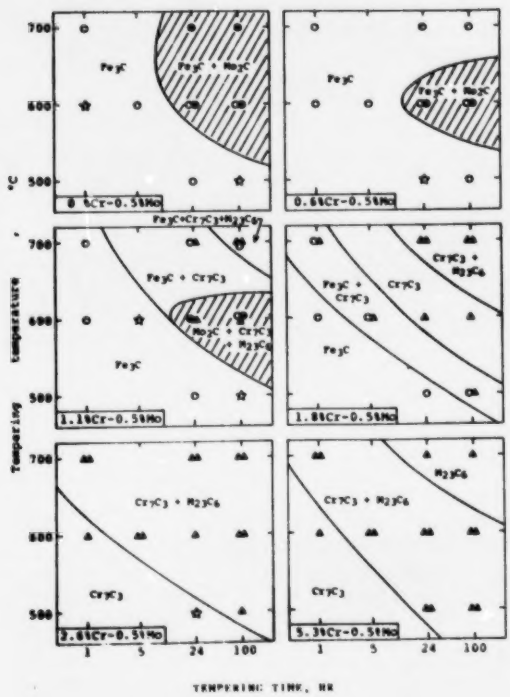


Fig. 8 - Carbide types present in Cr-0.5 Mo steels shown in the tempering-time diagram (17). (neg 14487)

Note: ° $Fe_3C$, ° $Mo_2C$, Δ $Cr_7C_3$, Δ $M_{23}C_6$, * no diffraction pattern.

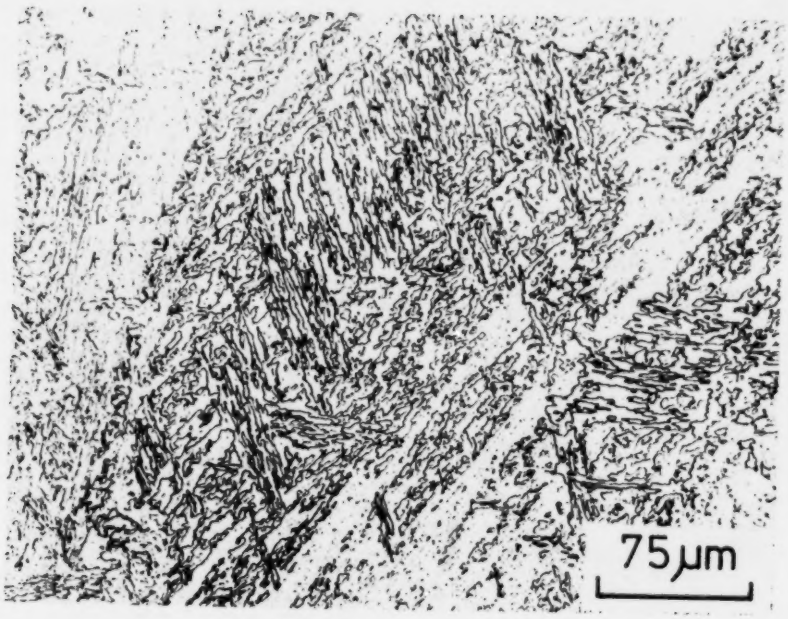


Fig. 9(a) - Elongated bainitic packets in 2.25 Cr-1 Mo SAW weld metal (12). (neg 13367)

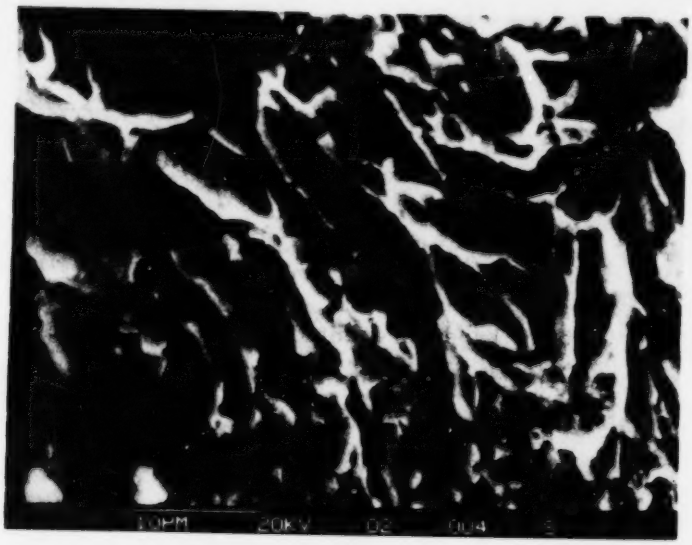

Fig. 9(b) - Fractured surface of 2.25 Cr-1 Mo SAW weld metal. Cleavage facet size corresponds to bainite packet dimensions. SEM fractograph (10). (neg 11908)

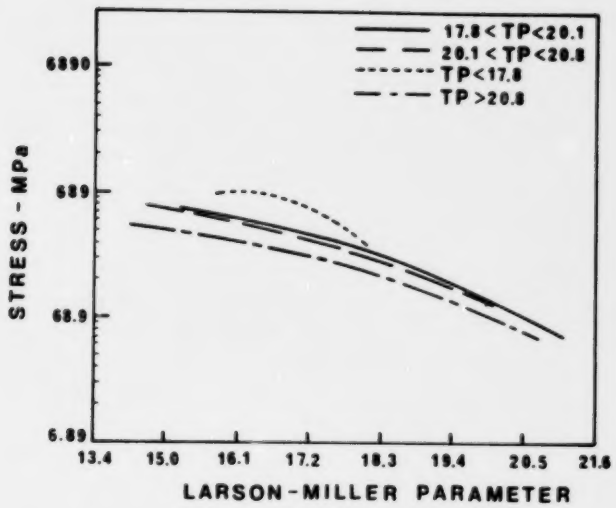


Fig. 10 - Stress rupture behaviour of 2.25 Cr-1 Mo SMA weld metal as a function of temper parameter (6). (neg 14484)